



A Journal of the Gesellschaft Deutscher Chemiker

Angewandte Chemie

GDCh

International Edition

www.angewandte.org

Accepted Article

Title: Pt and CuOx decorated TiO₂ photocatalyst for oxidative coupling of methane to C₂ hydrocarbons in a flow reactor

Authors: XIYI LI, Jijia Xie, Heng Rao, Chao Wang, and Junwang Tang

This manuscript has been accepted after peer review and appears as an Accepted Article online prior to editing, proofing, and formal publication of the final Version of Record (VoR). This work is currently citable by using the Digital Object Identifier (DOI) given below. The VoR will be published online in Early View as soon as possible and may be different to this Accepted Article as a result of editing. Readers should obtain the VoR from the journal website shown below when it is published to ensure accuracy of information. The authors are responsible for the content of this Accepted Article.

To be cited as: *Angew. Chem. Int. Ed.* 10.1002/anie.202007557

Link to VoR: <https://doi.org/10.1002/anie.202007557>

COMMUNICATION

Platinum and CuO_x-Decorated TiO₂ Photocatalyst for Oxidative Coupling of Methane to C₂ Hydrocarbons in a Flow Reactor

Xiyi Li, ^[a] Jijia Xie, ^[a] Heng Rao, ^[b, c] Chao Wang, ^[a] and Junwang Tang*^[a]

[a] X. Li, Dr. J. Xie, C. Wang, Prof. J. Tang
Solar Energy & Advanced Materials Research Group, Department of Chemical Engineering
University College London
Torrington Place, London, WC1E 7JE (UK)
E-mail: junwang.tang@ucl.ac.uk

[b] Dr. H. Rao
State Key Laboratory of Inorganic Synthesis and Preparative Chemistry, College of Chemistry
Jilin University
2699 Qianjin Street, Changchun, 130012 (China)

[c] Dr. H. Rao
International Center of Future Science, Jilin University
2699 Qianjin Street, Changchun, 130012 (China)
E-mail: rao@jlu.edu.cn

Supporting information for this article is given via a link at the end of the document. *(Please delete this text if not appropriate)*

Abstract: Oxidative coupling of methane (OCM) has been considered as one of the most promising and attractive catalytic technology to upgrade methane. However, C₂ products (C₂H₆/C₂H₄) from conventional methane conversion have not yielded commercially due to the competition from overoxidation and carbon accumulation at high temperatures. Herein, we reported the co-deposition of Pt nanoparticles and CuO_x clusters on TiO₂ (PC-50), and then used the photocatalyst to demonstrate the first successful case of photocatalytic OCM in a flow reactor operated at room temperature and under atmospheric pressure. The optimized Cu_{0.1}Pt_{0.5}/PC-50 sample showed a highest yield of C₂ product of 6.8 μmol h⁻¹, at the space velocity of 2400 h⁻¹, two times higher than the sum of the activity of Pt/PC-50 (1.07 μmol h⁻¹) and Cu/PC-50 (1.9 μmol h⁻¹), and it might also be the highest among photocatalytic methane conversions reported so far under atmospheric pressure. A high selectivity of 60% to C₂ was also comparable to the benchmark work of conventional high temperature (>943K) thermal catalysis. It is proposed that Pt functioned as an electron acceptor facilitating charge separation, while holes could transfer to CuO_x avoiding deep dehydrogenation and overoxidation of C₂ products. This work provides a new revenue for photocatalytic methane upgrade.

Under the pressure of the decreasing reserves of crude oil, natural gas (methane) is widely accepted as an alternative for fuel and more importantly as a fundamental building block for chemical synthesis.^[1] So far, only indirect conversion of methane via syngas (a certain ratio of H₂ and CO) process reaches feasible commercial-scale.^[2] This multi-stage process is not only energy-intensive, operated at a high temperature with high capital cost, but also accompanied by substantial CO₂ emission. Therefore, there are manifest financial and environmental incentives to explore the direct transformation of methane to value-added chemicals under moderate conditions.

Among various direct transformation technologies, oxidative coupling of methane (OCM) to ethane and ethylene has been regarded as a promising route for the valorisation of methane.^[3]

However, it is difficult to activate or convert CH₄ due to its inert nature, including high C-H bond energy (439 kJ mol⁻¹), symmetrical tetrahedral geometry, low polarizability (2.84 × 10⁻⁴⁰ C²·m²·J⁻¹).^[4] The introduction of oxygen and high temperature are thus conventionally required to overcome the thermodynamic barriers and increase the conversion. Such reaction conditions inevitably produce the undesired while thermodynamically favourable products, CO₂ and graphitic carbon. This subsequently leads to the low selectivity and low yield of C₂ products, bringing about a barrier to commercialization.

Photocatalysis, employing photons operated under mild conditions instead of thermal energy, has been regarded as a potential economic technology to break the thermodynamic barrier in the direct conversion of methane. Thus, the harsh reaction condition, overoxidation and deposition of coke could be theoretically avoided. In the past two decades, a wide range of products has been successfully obtained through photocatalytic methane conversion, such as methanol,^[5] ethanol,^[6] ethane/ethylene,^[7] benzene,^[8] syngas,^[9] and so on in batch reactors, but with very moderate efficiency due to the following major causes. Firstly, the high recombination rate of photo-induced carriers in the intrinsic semiconductor greatly limits their quantum efficiency, thus resulting in a low conversion. Next, the pristine photocatalysts with unmodified interface lead to poor selectivity because of overoxidation by the extremely oxidative photoholes in the valence band (VB) of the photocatalyst and the lack of active centres. More importantly, the majority of photocatalytic methane conversion reactions were carried out in batch reactors, which is easy to run but is theoretically hard to avoid overoxidation as the long residence time in the batch reactor favours the thermodynamically stable products of CO₂. In addition, such a system is also challenging for scale-up.

Herein, the co-modification of TiO₂ (PC-50) photocatalysts by Pt nanoparticles and CuO_x clusters were investigated to overcome the major drawbacks mentioned above for photocatalytic OCM. Furthermore, a flow system was applied to

COMMUNICATION

manipulate the residence time of the reactants at room temperature and atmospheric pressure. The synergy of Pt and Cu species on PC-50 led to an increased C_2 (ethane and ethylene) yield ($6.8 \mu\text{mol h}^{-1}$), which was ca. 3.5 times higher than the parent semiconductor PC-50. It is also the highest yield for C_2 products among all the photocatalytic methane conversion reported under atmospheric pressure. The C_2 selectivity of 60% was comparable to the traditional thermal catalysis operated at high temperature ($>943 \text{ K}$). The active species have then been investigated by X-ray photoelectron spectroscopy (XPS), Transmission electron microscopy (TEM), Electronic paramagnetic resonance (EPR), Photoluminescence (PL) spectroscopy, transient photocurrent response and in-situ EPR.

displayed no extra peaks for copper or platinum species, which was likely because of their low amount and/or high dispersion.^[10]

The anatase structure could be further supported by the Raman spectroscopy (Figure 1b). The typical Raman peaks for anatase TiO_2 were clearly observed at 144 cm^{-1} (E_g), 198 cm^{-1} (E_g), 399 cm^{-1} (B_{1g}), 512 cm^{-1} (A_{1g}) and 639 cm^{-1} (E_g), respectively.^[11] Notably, a slight blue shift and broadening of the 144 cm^{-1} Raman peak was observed after the introduction of co-catalysts, in particular $\text{Cu}_{0.1}\text{Pt}_{0.5}/\text{PC-50}$. This could be explained as the surface strain after surface modifications.^[12]

The photoabsorption properties of the as-prepared samples were investigated by Ultraviolet-visible diffuse reflectance spectroscopy (UV-Vis DRS). After the introduction of CuO_x clusters, the photo absorption enhanced in the range from 200 to 320 nm (Figure 2a). This was likely because of charge transfer between oxygen and isolated copper(II) species and the charge transfer in clusters.^[13] The absorption edge remained almost unchanged for all of the samples, indicating the intact band structure of PC-50 and the little contribution from CuO_x absorption.

The photocatalytic activities of the as-prepared samples for OCM were evaluated in a flow system at room temperature and under atmospheric pressure. It has been widely reported that the photo-induced holes at the valance band of TiO_2 tended to promote the mineralize CH_4 into CO_2 through deep dehydrogenation.^[14] The valence band edge of CuO and Cu_2O were around 0.75 eV and 0.99 eV more negative (vs. NHE) compared with TiO_2 , respectively.^[15] It indicates a potential to C_2 products rather than CO_2 after the introduction of copper species, because copper species were expected to accept the photo-induced holes from TiO_2 and dramatically lower their oxidation potential. Moreover, Cu^{II} clusters as active sites has previous observed to selectively oxidise methane in thermal catalysis.^[16,17] The optimum content of copper was first investigated (Figure 2b). It exhibited the volcanic trend with an increasing weight percentage of Cu and achieved the highest C_2 yield over $\text{Cu}_{0.1}/\text{PC-50}$ ($1.2 \mu\text{mol h}^{-1}$). This was probably because excessive amount of CuO could act as the recombination center of photo-induced electrons and holes,^[18] more discussion will be given later. After optimised Cu amount was obtained, Pt was added to facilitate charge separation as a widely known electron acceptor.^[19] In order to test the photocatalytic efficiency at a relatively harsh condition, we increased the space velocity from 1200 h^{-1} to 2400 h^{-1} and then the samples with bimetallic co-catalyst were investigated (Figure 2c and Figure S8). The conversion of methane was increased compared with the pristine TiO_2 while the yield of both C_2 products and CO_2 increased after the co-deposition of Pt nanoparticles and CuO_x clusters. This was due to more available separated photo-induced carriers through the efficient transfer of electrons and holes to Pt and CuO_x clusters, respectively. It should be noted that the selectivity to C_2 products firstly increased compared with selectivity to CO_2 with the increasing Pt on the Pt and CuO_x co-loaded samples. However, over-increasing Pt would cause a reduction of both yield and selectivity to C_2 products. The yield of C_2 products on the optimised sample $\text{Cu}_{0.1}\text{Pt}_{0.5}/\text{PC-50}$ was $6.8 \mu\text{mol h}^{-1}$, more than 2 times higher than the sum of $\text{Pt}_{0.5}/\text{PC-50}$ ($1.07 \mu\text{mol h}^{-1}$) and $\text{Cu}_{0.1}/\text{PC-50}$ ($1.9 \mu\text{mol h}^{-1}$), indicating the importance of the synergistic effect. Moreover, the yield of CO_2 only increased by around 20% compared with PC-50, indicating the indispensable role of CuO_x clusters in shifting selectivity to C_2 . Remarkably, this yield was about four times higher than the reported production

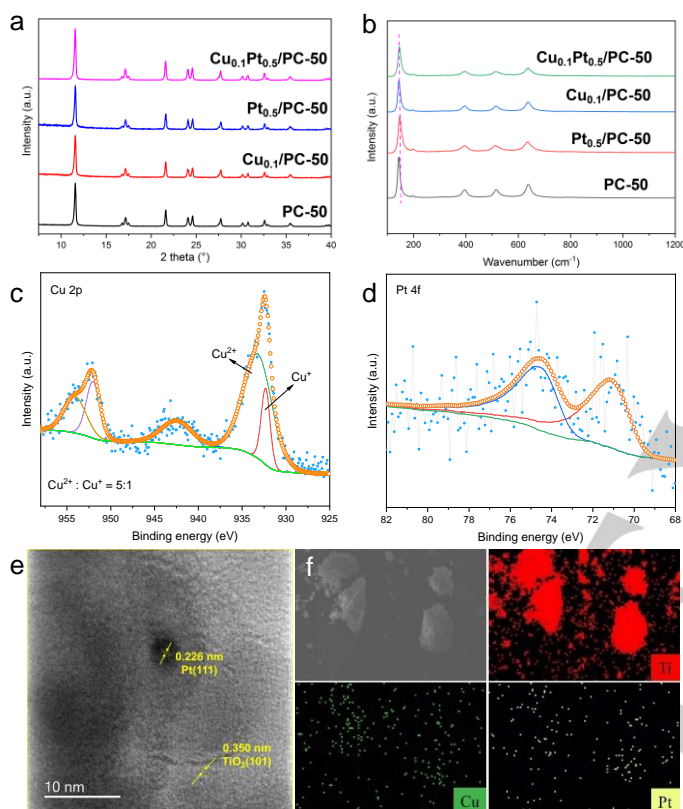


Figure 1. a) PXRD and b) Raman spectra of $\text{Cu}_{0.1}\text{Pt}_{0.5}/\text{PC-50}$, $\text{Pt}_{0.5}/\text{PC-50}$, $\text{Cu}_{0.1}/\text{PC-50}$ and PC-50 ; c) Cu 2p XPS spectra of $\text{Cu}_{0.1}/\text{PC-50}$; d) Pt 4f XPS spectra of $\text{Cu}_{0.1}\text{Pt}_{0.5}/\text{PC-50}$; e) HR-TEM images of $\text{Cu}_{0.1}\text{Pt}_{0.5}/\text{PC-50}$; f) EDX elemental mappings (Ti, Cu and Pt) of $\text{Cu}_{0.1}\text{Pt}_{0.5}/\text{PC-50}$.

TiO_2 has been regarded as one of the benchmark photocatalysts due to its intrinsically high stability and activity under UV photons. Thus commercial anatase TiO_2 (PC-50) was selected as a starting substrate. Then Pt nanoparticles and CuO_x species were introduced by photodeposition and subsequent wet impregnation method (for more details on material synthesis see the SI). The as-prepared sample was marked as $\text{Cu}_x\text{Pt}_y/\text{PC-50}$, where x and y represented the nominal weight ratio of Cu and Pt to PC-50, respectively. $\text{Cu}_{0.1}/\text{PC-50}$, $\text{Pt}_{0.5}/\text{PC-50}$ and PC-50 were the reference samples.

The crystal structures of all the as-prepared samples were indexed to anatase TiO_2 (JCPDS no. 84-1286), as shown in Powder X-ray Diffraction (PXRD) spectra (Figure 1a). After the introduction of Pt and Cu, the PXRD spectra remained unchanged, indicating the stable framework. Additionally, the spectra

COMMUNICATION

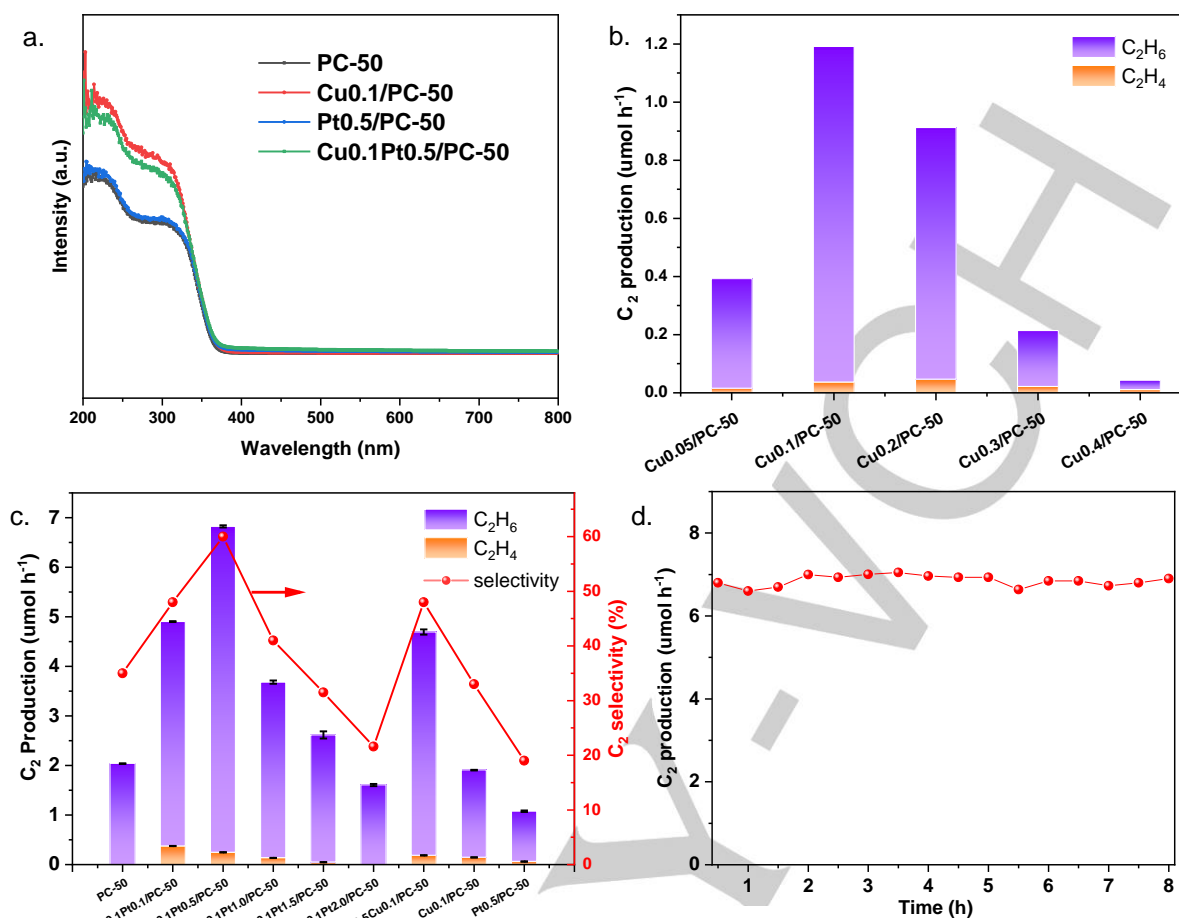


Figure 2. a) UV-DRS spectra of Cu_{0.1}Pt_{0.5}/PC-50, Pt_{0.5}/PC-50, Cu_{0.1}/PC-50 and PC-50; b) C₂ Production of photocatalytic OCM over Cu_x/PC-50 (x = 0.05, 0.1, 0.2, 0.3, 0.4). (Reaction condition: O₂ : CH₄ = 1 : 240, GHSV = 1200 h⁻¹, 10% of CH₄, 365 nm LED 20 W, 40 °C); c) C₂ production and selectivity of photocatalytic OCM over Cu_{0.1}Pt_y/PC-50 (y = 0.1, 0.5, 1.0, 1.5, 2.0 wt%), Cu_{0.1}/PC-50, PC-50, Pt_{0.5}/PC-50 and Pt_{0.5}Cu_{0.1}/PC-50; (Reaction condition: O₂ : CH₄ = 1 : 400, GHSV = 2400 h⁻¹, 10% of CH₄, 365 nm LED 40 W, 40 °C); d) Stability test of photocatalytic OCM over Cu_{0.1}Pt_{0.5}/PC-50.

rate of C₂H₆ and C₂H₄ by photocatalytic methane conversion with an irradiation of > 300 nm over different catalysts under atmospheric pressure (Table S2). Given that some reactions in Table S2 were non-oxidative coupling of methane, their yields were relatively low due to the high thermodynamic barriers.^[20] The yield of C₂ products over our optimised sample was also higher compared with the partial oxidation of methane. Furthermore, the selectivity towards C₂ products of 60% was comparable to the traditional catalysts (e.g. Li/MgO) operated at high temperature (>943 K).^[3,21] We also calculated the apparent quantum yield (AQE) based on the methane conversion for Cu_{0.1}Pt_{0.5}/PC-50 and PC-50. The AQE of Cu_{0.1}Pt_{0.5}/PC-50 (0.5% at 365 nm) was nearly two times higher than that of PC-50 (0.25% at 365 nm), indicating the higher utilization of light energy. The further adding of Pt led to decreased C₂ selectivity and increased CO₂ yield with the highest CO₂ yield reaching 11.6 μmol h⁻¹. We believe too many Pt nanoparticles might lead to the excessive formation of O₂⁻, which was the major component for overoxidation.^[22] Accordingly, Pt_{0.5}/PC-50 only exhibited increased yield of CO₂ while the lowest yield of C₂ products compared with PC-50. This resulted in the highest selectivity to CO₂ (ca. 80%) again due to the increasing available photo-induced electrons for O₂⁻ generation and strong oxidative holes at the valence band of TiO₂. The preparation order of two co-catalysts was changed to observe its effect. Another photocatalyst Pt_{0.5}Cu_{0.1}/PC-50 was thus prepared. Interestingly, it

showed a decreased C₂ yield (4.7 μmol h⁻¹) compared with Cu_{0.1}Pt_{0.5}/PC-50, indicating that the deposition sequence of co-catalysts also had an important influence on the performance. The function of Pt was believed to accept photo-induced electrons and help charge separation. If the CuO_x clusters were firstly deposited, some of them would block the contact between Pt particles and TiO₂, leading to reduced charge separation effect, thus lower the conversion and yield. It was noted that the yield of C₂ products over Cu_{0.1}/PC-50 was lower than that of PC-50, while the yield of CO₂ was similar. As proved by the XPS results later, the copper species in our samples was mainly CuO. Its conduction band (CB) was 0.75 eV more positive than that of TiO₂. Taking into account the more negative VB of CuO than that of TiO₂, some holes transferred from the VB of TiO₂ would recombine with the electrons from the CB of TiO₂ on the CuO_x clusters. This could lead to the decreased generation of methyl radicals, which would have a more negative effect on the coupling to C₂ species than deep oxidation to CO₂ because of the second-order nature of the coupling reaction to C₂ products.^[23] While some remaining highly oxidative holes with the O₂⁻ formed by the remaining electrons continued to proceed the overoxidation of methane to CO₂. Thus, the yield of CO₂ exhibited nearly no change while the yield of C₂ products decreased after single introduction of CuO_x clusters, indicating the important role of Pt nanoparticles for the synergistic effect. Please note in our system, only ethane, ethylene and CO₂

COMMUNICATION

as products could be detected by our GC equipped with a methanizer unit and a FID detector (Figure S7). Thus, the C_2 selectivity mentioned above was calculated based on the measured products. No products could be detected when the reaction was carried out in the absence of methane or without light irradiation (Table S1). This confirmed that it was a photocatalytic process with CH_4 as the only carbon source.

The stability of the optimised sample $Cu_{0.1}Pt_{0.5}/PC-50$ was then tested. No decay of C_2 yield except slight fluctuation could be observed during 8 h reaction (Figure 2d). The structure of catalysts and the chemical states of active species also remained unchanged during the reaction (Figure S5, S6). This indicated that $Cu_{0.1}Pt_{0.5}/PC-50$ exhibited excellent stability under photocatalytic OCM process.

XPS was then conducted to analyse the chemical states of co-catalysts on the optimum catalyst (Figure 1c, d; Figure S2, 3). Due to the extremely low loading amount of copper species, no clear Cu 2p peak could be observed on $Cu_{0.1}Pt_{0.5}/PC-50$ (Figure S3). Thus, a sample ($Cu_{2.0}/PC-50$), prepared with the same procedure but large loading amount of copper species, was used to identify the chemical states of Cu on PC-50 (Figure 1c). The peaks attributed to Cu 2p_{3/2} and Cu 2p_{1/2} at around 933.4 eV and 953.9 eV, coupling with the shake up satellite peak at around 942.6 eV, indicated the main existence of fully oxidised CuO.^[24] In addition, a small amount of Cu(I) (Cu(II) : Cu(I) = 5 : 1) could be found with peaks at 932.2 eV and 952 eV, respectively. It was believed that similar species were formed on the best sample, $Cu_{0.1}Pt_{0.5}/PC-50$. Compared with PC-50 and $Pt_{0.5}/PC-50$, the binding energy of Ti 2p_{3/2} transition shifted to lower binding energy over $Cu_{0.1}/PC-50$ and $Cu_{0.1}Pt_{0.5}/PC-50$ (Figure S2). The lower binding energy suggested the electrons probably transferred from Cu to Ti, indicating the interaction between the co-catalysts and PC-50.^[25] XPS analysis of Pt provided the peaks at 71.2 eV and 74.6 eV, which was assigned to metallic states.^[26]

TEM and HRTEM images were provided to further investigate the particle size and distribution of $Cu_{0.1}Pt_{0.5}/PC-50$. Some nanoparticles were dispersed on PC-50 with diameters from 3.5 to 6 nm (Figure S4). These nanoparticles were further identified with HRTEM (Figure 1e), in which the d-spacing of lattice fringes could be attributed to Pt (111, 0.226 nm) and anatase TiO₂ (101, 0.350 nm), respectively.^[27] The copper species have not been observed at this resolution, suggesting the existence of smaller clusters. The Energy Dispersive X-ray (EDX) mapping showed that Cu and Pt dispersed homogeneously (Figure 1f), in good agreement with the XRD results.

In order to further unravel the chemical state of copper species and the charge transfer, in-situ EPR was carried out (Figure 3a). Compared with $Pt_{0.5}/PC-50$, $Cu_{0.1}Pt_{0.5}/PC-50$ exhibited new spectra corresponding to CuO hyperfine structure owing to $I = 3/2$ of Cu(II), indicating the existence of Cu(II) in the copper species.^[28] Although the existence of long-range dipolar interactions between different Cu(II) sites resulted in the broadening of spectral lines, the anisotropic hyperfine structure could be found after careful analysis. $g_{\parallel} = 2.395$ with $A_{\parallel} \approx 100$ G was obtained, while the value for $g_{\perp} = 2.05$ could not be resolved. These resonance parameters were in agreement with the distorted octahedral coordination of Cu(II) ions in CuO clusters.^[29] This result suggested the existence of a high distribution of CuO clusters, which explained the invisible copper species in HRTEM. This result was also consistent with the Cu 2p XPS analysis. Upon

365 nm LED illumination, the intensity of Cu(II) signal was expected to decrease if it could accept electrons to form EPR silent Cu(I) sites.^[29] However, the spectrums under the chopped

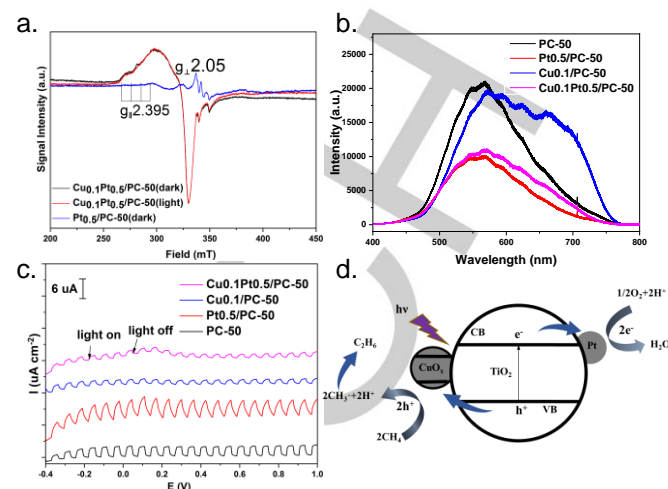


Figure 3. a) EPR spectra of $Cu_{0.1}Pt_{0.5}/PC-50$ (light on and light off) and $Pt_{0.5}/PC-50$ (light on); b) PL spectra of $Cu_{0.1}Pt_{0.5}/PC-50$, $Pt_{0.5}/PC-50$, $Cu_{0.1}/PC-50$ and $PC-50$; c) Photocurrent of $Cu_{0.1}Pt_{0.5}/PC-50$, $Pt_{0.5}/PC-50$, $Cu_{0.1}/PC-50$ and $PC-50$; d) The proposed photocatalytic OCM process over $Cu_{0.1}Pt_{0.5}/PC-50$.

light were almost overlapped, indicating the photo-induced electrons were trapped by Pt rather than the CuO sites as presented in Figure 3d. Thus, the introduction of Pt was important to impede the charge recombination on CuO_x clusters, resulting in improved performance of $Cu_{0.1}Pt_{0.5}/PC-50$.

The facilitation of charge transfer was further investigated by PL spectra (Figure 3b). An obvious band could be observed for the pristine PC-50, while the PL intensity decreased notably after the incorporation of Pt nanoparticles. This suggested the efficient separation of photo-induced electrons and holes by Pt nanoparticles. In the case of $Cu_{0.1}/PC-50$, a photoluminescence spectrum with fine structure was shown, which could be attributed to the highly dispersed copper species.^[30] According to the UV-vis DRS result, it was suggested that the photoexcitation occurred by charge transfer from oxygen to copper in the clusters. Considering the enhanced absorption in UV region observed in UV-vis DRS spectra and the larger enhanced emission in the PL spectra, the photo-induced carriers in PC-50 probably recombined in the CuO_x clusters over $Cu_{0.1}/PC-50$. This was also consistent with the analysis of the band structure mentioned above and in Figure 3d. More importantly, the PL intensity of $Cu_{0.1}Pt_{0.5}/PC-50$ was obviously lower than that of $Cu_{0.1}/PC-50$, indicating that the photo-induced electrons in PC-50 were transferred to Pt rather than to the CB of CuO_x clusters.

The function of Pt as an electrons sink was further consolidated by the transient photocurrent response (Figure 3c). Compared with pristine PC-50, $Pt_{0.5}/PC-50$ exhibited higher reduction photocurrent density because of the efficient transfer of electrons to Pt nanoparticles. While the introduction of copper species resulted in lower photocurrent response for both $Cu_{0.1}/PC-50$ and $Cu_{0.1}Pt_{0.5}/PC-50$. As mentioned above, the valence band of CuO or Cu_2O were less positive than TiO₂. This decay of photocurrent density could be explained by the weak oxidative potential of photo-induced holes on CuO_x clusters.^[15]

Based on the above characterisations and investigations, a probable mechanism of photocatalytic OCM over $Cu_{0.1}Pt_{0.5}/PC-50$

COMMUNICATION

was proposed (Figure 3d). Upon light irradiation, electrons could be excited from the VB of PC-50 to its CB and then migrated to Pt, while holes could be transferred to the VB of CuO_x clusters. This process not only retarded the recombination of photo-induced electrons and holes, but also lower the oxidation potential of photo-induced holes to avoid deep dehydrogenation and overoxidation. The C-H bond in CH₄ molecules was abstracted by the holes in the VB of CuO_x clusters to form methyl radicals and protons. The combination of methyl radicals formed the ethane molecules and the deep dehydrogenation could lead to the formation of ethylene. O₂ could be reduced by electrons from Pt nanoparticles to form O₂^{•-} and the protons could be removed by O₂^{•-} to form water. The synergy effects between Pt and CuO_x clusters at reduction sites and oxidation sites respectively were highlighted to complete the catalytic cycle.

In summary, we reported the first example of a continuous photocatalytic OCM process at room temperature and atmospheric pressure in a flow system. The Pt nanoparticles and CuO_x clusters were introduced to PC-50 via photodeposition and wet impregnation methods, respectively. The separation of photo-induced e⁻/h⁺ was facilitated and the oxidation potential of holes was lowered to avoid overoxidation, leading to high yield and selectivity towards C₂ hydrocarbons. The synergy of Pt nanoparticles and CuO_x clusters resulted in the increased C₂ yield (6.8 μmol h⁻¹), which was ca. 3.5 times higher than PC-50 and more than two times higher than the sum of the activity of Pt/PC-50 (1.07 μmol h⁻¹) and Cu/PC-50 (1.9 μmol h⁻¹), respectively, resulting into a AQE of 0.5% at 365 nm. The selectivity of 60% was also comparable to traditional OCM thermal catalysts and such high photocatalytic activity remained stable after a long time run. Overall this work contributes to an effective green route to methane upgrade.

Acknowledgements

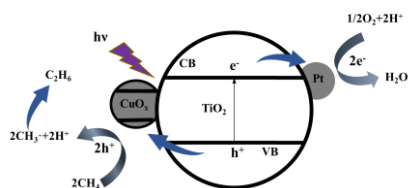
X. Li, J. Xie, C. Wang and J. Tang are thankful for financial support from RS International Exchanges 2017 Cost Share Award (IECNSFC170342), UK EPSRC (EP/N009533/1), Royal Society-Newton Advanced Fellowship grant (NA170422) and the Leverhulme Trust (RPG-2017-122). We are also thankful for the EPR characterisations from Yiyun Liu. X. Li would like to acknowledge UCL PhD studentship (GRS and CRS). H. Rao is thankful for the 111 Project (Grant No. B17020) and also acknowledges the financial supports from the National Natural Science Foundation of China (Grant No. 21905106).

Keywords: OCM • methane conversion • photocatalysis • flow reactor • C₂H₄/C₂H₆

- [1] P. Schwach, X. Pan, X. Bao, *Chem. Rev.* **2017**, *117*, 8497–8520.
 [2] Y. Xu, X. Bao, L. Lin, *J. Catal.* **2003**, *216*, 386–395.
 [3] B. L. Farrell, V. O. Igenegbai, S. Linic, *ACS Catal.* **2016**, *6*, 4340–4346.
 [4] P. Tang, Q. Zhu, Z. Wu, D. Ma, *Energy Environ. Sci.* **2014**, *7*, 2580–2591.
 [5] J. Xie, R. Jin, A. Li, Y. Bi, Q. Ruan, Y. Deng, Y. Zhang, S. Yao, G. Sankar, D. Ma, et al., *Nat. Catal.* **2018**, *1*, 889–896.
 [6] Y. Zhou, L. Zhang, W. Wang, *Nat. Commun.* **2019**, *10*, 506.
 [7] L. Yuliati, H. Yoshida, *Chem. Soc. Rev.* **2008**, *37*, 1592–1602.
 [8] L. Li, S. Fan, X. Mu, Z. Mi, C.-J. J. Li, *J. Am. Chem. Soc.* **2014**, *136*, 7793–7796.
 [9] L. Zhou, J. M. P. Martinez, J. Finzel, C. Zhang, D. F. Swearer, S. Tian, H. Robotjazi, M. Lou, L. Dong, L. Henderson, et al., *Nat. Energy* **2020**, *5*, 61–70.
 [10] X. Li, Y. Pi, Q. Xia, Z. Li, J. Xiao, *Appl. Catal. B Environ.* **2016**, *191*, 192–201.
 [11] T. Ohsaka, F. Izumi, Y. Fujiki, *J. Raman Spectrosc.* **1978**, *7*, 321–324.
 [12] W. S. Li, Z. X. Shen, H. Y. Li, D. Z. Shen, X. W. Fan, *J. Raman Spectrosc.* **2001**, *32*, 862–865.
 [13] M. Shimokawabe, H. Asakawa, N. Takezawa, *Appl. Catal.* **1990**, *59*, 45–58.
 [14] L. Yu, Y. Shao, D. Li, *Appl. Catal. B Environ.* **2017**, *204*, 216–223.
 [15] Y. Xu, M. A. A. Schoonen, *Am. Mineral.* **2000**, *85*, 543–556.
 [16] S. Grundner, W. Luo, M. Sanchez-Sanchez, J. A. Lercher, *Chem. Commun.* **2016**, *52*, 2553–2556.
 [17] V. L. Sushkevich, D. Palagin, M. Ranocchiar, J. A. Van Bokhoven, *Science (80-.)* **2017**, *356*, 523–527.
 [18] Y. Zhang, Y. Hu, J. Zhao, E. Park, Y. Jin, Q. Liu, W. Zhang, *J. Mater. Chem. A* **2019**, *7*, 16364–16371.
 [19] A. Kudo, Y. Miseki, *Chem. Soc. Rev.* **2009**, *38*, 253–278.
 [20] H. Song, X. Meng, Z. Wang, H. Liu, J. Ye, *Joule* **2019**, *3*, 1606–1636.
 [21] S. Arndt, G. Laugel, S. Levchenko, R. Horn, M. Baerns, M. Scheffler, R. Schlögl, R. Schomäcker, *Catal. Rev.* **2011**, *53*, 424–514.
 [22] S. G. Kumar, L. G. Devi, *J. Phys. Chem. A* **2011**, *115*, 13211–13241.
 [23] Y. S. Su, J. Y. Ying, W. H. Green, *J. Catal.* **2003**, *218*, 321–333.
 [24] J. Li, J. Zeng, L. Jia, W. Fang, *Int. J. Hydrogen Energy* **2010**, *35*, 12733–12740.
 [25] J. Xia, N. Masaki, K. Jiang, S. Yanagida, *J. Phys. Chem. B* **2006**, *110*, 25222–25228.
 [26] S. Sorcar, Y. Hwang, J. Lee, H. Kim, K. M. Grimes, C. A. Grimes, J.-W. Jung, C.-H. Cho, T. Majima, M. R. Hoffmann, et al., *Energy Environ. Sci.* **2019**, *12*, 2685–2696.
 [27] S. Farsinezhad, H. Sharma, K. Shankar, *Phys. Chem. Chem. Phys.* **2015**, *17*, 29723–29733.
 [28] I. Ardelean, M. Peteanu, R. Ciceo-Lucacel, I. Bratu, *J. Mater. Sci. Mater. Electron.* **2000**, *11*, 11–16.
 [29] G. Li, N. M. Dimitrijevic, L. Chen, T. Rajh, K. A. Gray, *J. Phys. Chem. C* **2008**, *112*, 19040–19044.
 [30] H. Yoshida, M. G. Chaskar, Y. Kato, T. Hattori, *Chem. Commun.* **2002**, *2*, 2014–2015.

COMMUNICATION

Entry for the Table of Contents



Pt nanoparticles and CuO_x clusters co-decorated TiO_2 for photocatalytic OCM in a flow system at room temperature and atmospheric pressure has been achieved, resulting into the highest yield rate of $6.8 \mu\text{mol h}^{-1}$ to C_2 hydrocarbons with excellent selectivity (60%) operated at the space velocity of 2400 h^{-1} .